

A new spectrally sharpened sensor basis to predict color naming, unique hues, and hue cancellation

Javier Vazquez-Corral*

Computer Science Department, Universitat Autònoma de Barcelona and Computer Vision Center, 08193, Cerdanyola del Vallès, Spain



J. Kevin O'Regan

Laboratoire Psychologie de la Perception - CNRS UMR 8158, Université Paris Descartes, 45 Rue des Saints Pères, 75006, Paris, France



Maria Vanrell

Computer Science Department, Universitat Autònoma de Barcelona and Computer Vision Center, 08193, Cerdanyola del Vallès, Spain



Graham D. Finlayson*

School of Computing Sciences, University of East Anglia, Norwich, NR4 7TJ, United Kingdom



When light is reflected off a surface, there is a linear relation between the three human photoreceptor responses to the incoming light and the three photoreceptor responses to the reflected light. Different colored surfaces have different such linear relations. Recently, Philipona and O'Regan showed that when this relation is singular in a mathematical sense, then the surface is perceived as having a highly nameable color. Furthermore, white light reflected by that surface is perceived as corresponding precisely to one of the four psychophysically measured unique hues. However, Philipona and O'Regan's approach seemed unrelated to classical psychophysical models of color constancy.

In this paper we make this link. We begin by transforming cone sensors to spectrally sharpened counterparts. In sharp color space, illumination change can be modeled by simple von Kries type scalings of response values within each of the spectrally sharpened response channels. In this space, PO's linear relation is captured by a simple Land-type color designator defined by dividing reflected light by incident light. This link between PO's theory and Land's notion of color designator gives the model biological plausibility.

We then show that Philipona and O'Regan's singular surfaces are surfaces which are very close to activating only one or only two of such newly defined spectrally sharpened sensors, instead of the usual three. Closeness to zero is quantified in a new simplified measure of singularity which is also shown to relate to the chromaticness of colors. As in PO's original work, our new theory accounts of a large variety of psychophysical color data.

Keywords: sensor sharpening, color naming, unique hues, hue cancellation. *: Corresponding authors

Introduction

The human brain treats colors asymmetrically: as regards colored lights, certain hues of red, green, yellow, and blue, the so-called "unique hues" (Valberg, 2001), are perceived as being more "pure" than other hues; as regards colored surfaces, the well-known "World Color Survey" (WCS) shows that certain colors are considered more basic or prototypical or "focal" across different cultures (red, yellow, green, and blue being the four most frequent) (Berlin & Kay, 1969), (Kay, 2005).

Explanations for these facts cannot lie in the physical light spectra or reflectance properties, because these are continuous functions with no intrinsic asymmetries. **Equally, appealing to the fact that there are three cone types does not in any obvious way by itself predict the experimentally observed asymmetries.** Thus, explanations must be sought in neural (Parraga, Troscianko, & Tolhurst, 2002), environmental (Yendrikhovskij, 2001), cultural, or linguistic mechanisms (Kay & Regier, 2003).

It seems at first sight that a plausible candidate for a neural mechanism might lie in the opponent color proc-

essing carried out by the early visual system (Hering, 1891), (Wyszecki & Stiles, 1982). However unfortunately the extremes of the red/green and blue/yellow axes proposed in the opponent theory do not correspond to the four unique hues. In particular, the theory would predict that to appear as unique “green”, a light should only activate the red/green channel, and not the blue/yellow channel. Yet it is found that to appear uniquely green a light must contain some yellow. Likewise it is found that to appear uniquely yellow, some red must be mixed in; to appear uniquely blue, some green must be mixed in (Burns, Elsner, Pokorny, & Smith, 1984), (Cicerone, Krantz, & Larimer, 1975), (Kuehni, 2004), (Mollon & Jordan, 1997), (Valberg, 2001) (Webster, Miyahara, Malkoc, & Raker, 2000), (Wuerger, Atkinson, & Cropper, 2005).

Perceptual saliency of colors is another mechanism that has been invoked, this time to explain the intercultural data of the World Color Survey concerning the naming of surface colors. The idea is that speakers distribute color names over perceptual color space in a way to maximize the perceptual similarity between colors having the same names, and to minimize the similarity between colors having different names (Kay & Regier, 2003). Whereas this model does a reasonable job of explaining the boundaries between different color names, it provides no explanation for the exact hues which are considered to be “focal”.

Recently, Philipona and O'Regan (from now on PO) (Philipona & O'Regan, 2006) defined a new approach for explaining the unique hues and intercultural World Color Survey naming data. **PO follow a very simple idea already implicit in the color literature: color should be considered to be the biological analogue of what physicists call surface reflectance.** PO take the physicist's notion of reflectance, and create a biological reflectance function which can be used by the brain with its three broad-band sensors. They calculate this biological reflectance function for a wide variety of surfaces and discover that certain surfaces have the mathematical property of being “singular”. What this means is that these surfaces take incoming light, which usually can vary in a 3-dimensional space defined by L, M, and S cone activations, and transform it into light which varies only in either a 2- or in a 1-dimensional subspace of the LMS activation space. Because singular surfaces reduce variability from three dimensions to two or one dimension, they can be said to display a simpler behaviour as concerns how they affect incoming light than the majority of surfaces. What is now extremely striking is that these singular surfaces turn out to be almost exactly the red, yellow, green, and blue surfaces most frequently observed to be focal. Furthermore, if these surfaces are illuminated by a canonical source of natural illumination (Illuminant D65), the hues of the resulting reflected light correspond accurately to the monochromatic lights widely considered to be “unique” in psychophysical experiments.

A strength of the PO approach is that it provides these explanations for both naming data and unique hues without any parameter adjustments. Well-known results on hue cancellation and hue equilibrium (Chichilnisky & Wandell, 1999), (Jameson & Hurvich, 1955) also fall out very exactly from the predicted unique hue data.

A weakness of the PO approach up until now has been the fact that no clear link has been made with classical approaches in color psychophysics, physiology, or in artificial vision. In the present paper we remedy this by showing that the PO approach is closely related to the notion of spectral sharpening used in computational vision to obtain improved color constancy. The idea is that to characterize surface reflectivity in a way that is independent of illuminant, it is advantageous to use, not the normal three cone sensors of the human eye, but “sharpened” sensors which are linear combinations of the cone mechanisms. The sharp sensors allow us to define surface color “designators” similar to those suggested by Land in his retinex theory (Land, 1964) (color designators are the color response for a surface divided by the color response to white). The sharp designators defined by our approach have the property that they are much more independent of illumination than those defined in Land's approach. Furthermore, our sharp color designators turn out to be essentially the same as the biological reflectances defined by PO. **Importantly, to compute the sharp designator we do not need to know what reflectance we are looking at: we simply divide the sharpened sensor responses of the (unknown) surface by the sharpened sensor responses of white. This is in contradistinction to the original PO theory where knowledge of the surface is required to calculate the biological reflectance coefficients. Removing the requirement that “we know what we are looking at” is a significant contribution of this paper.**

An additional contribution of our paper is to improve the measure of singularity used by PO. Our new measure provides an appealing, perceptually reasonable link to the notion of chromaticness, that is, the degree to which a light deviates from grey. We show that using our new measure of singularity, predictions of color naming and unique hues can be obtained that are at least as and possibly more precise than those obtained by PO.

The paper is organized as follows. In section (2) we explain the biological model of PO. After this, in section (3) we define our model based on a set of sharp sensors and a new compact singularity index. This is followed by section (4) where we summarize the different results obtained.

Philipona and O'Regan biological model

PO's biological model (Philipona & O'Regan, 2006) is built on the assumption that the human vision system

must attempt to extract the reflection properties of surfaces in the world independently of ambient lighting conditions. In other words, it must try to deliver a canonical, biological representation of reflectance.

Physicists achieve this task by defining the notion of “reflectance function” linking incident light energy at a particular wavelength to reflected light energy at that wavelength. Because the majority of surfaces only absorb or reflect light energy at a given wavelength, and do not redistribute energy in other wavelengths, physicists can define reflectance at a given wavelength λ as a scalar $s(\lambda)$ attenuation between 0 and 1, and write a simple linear relation linking incident light energy $e(\lambda)$ at wavelength λ to reflected light energy $p(\lambda)$ at that wavelength:

$$p(\lambda) = s(\lambda)e(\lambda), \quad \text{giving} \quad s(\lambda) = p(\lambda) / e(\lambda) \quad (1)$$

so that the physical reflectance of a surface is simply the ratio of reflected to incident light at each wavelength.

Unlike physicists, who can measure energy at each monochromatic wavelength using a spectroradiometer, information accessible to the brain is blurred over the breadth of wavelengths that the human L, M, and S cone types are sensitive to. It is now no longer true that the effect of the surface on incident light can be expressed simply as an attenuation of energy within each of these broad bands. However, PO show that it is still possible to define a “biological” reflectance measure that links the information accessible to the brain about the incident light, to the information accessible to the brain about the reflected light in a way analogous to physicists’ equation (1).

The information accessible to the brain about an illuminant $e(\lambda)$ is the vector corresponding to the responses of the three cone types to that illuminant:

$$\underline{w}^e = (w_1^e, w_2^e, w_3^e)^t$$

$$\text{where } w_i^e = \int_{\psi} Q_i(\lambda)e(\lambda)d\lambda, \quad i = 1, 2, 3 \quad (2)$$

here t denotes the transpose of the vector, $Q_i(\lambda)$ for $i=1,2,3$ define the absorption of the three human cone types at each wavelength λ , and we integrate over the visible spectrum ψ .

The information accessible to the brain about the reflected light is the vector corresponding to the responses of the three cone types to the reflected light from the surface:

$$\underline{p}^{s,e} = (p_1^{s,e}, p_2^{s,e}, p_3^{s,e})^t$$

$$\text{where } p_i^{s,e} = \int_{\psi} Q_i(\lambda)e(\lambda)S(\lambda)d\lambda, \quad i = 1, 2, 3 \quad (3)$$

Where $S(\lambda)$ is the physicist's reflectance function for the surface s .

PO now show the at first sight surprising result that for any surface $s(\lambda)$ there exists a 3×3 matrix A^s which is independent of the illuminant e and very accurately describes the way the surface transforms the accessible information about any incident light into the accessible information about reflected light:

$$\forall(e), \quad \underline{p}^{s,e} \approx A^s \underline{w}^e \quad (4)$$

A^s is the 3×3 matrix best taking $\underline{p}^{s,e}$ (for any illuminant e) to \underline{w}^e in a least-squares sense. PO studied the validity of such an equation for a very large number of natural and artificial illuminants, and for a very large number of colored surfaces. In fact, the result is analytically true if incoming illumination is of dimensionality 3, that is, if it can be described as a weighted sum of three basis functions (Philipona & O'Regan, 2006). Since this is known to be true to a good approximation for Daylights (Judd et al., 1964), the equation is very accurate.

Equation (4) is the biological analogue of the physicists relation (1), but because it is written in terms of vectors and matrices instead of scalars, PO could not immediately invert it by dividing the vector $\underline{p}^{s,e}$ by the vector \underline{w}^e to obtain the biological equivalent of the physicist's reflectance in equation (1). PO were able to do something similar however by first diagonalizing the matrix A^s , that is, writing it as the product $(T^s)^{-1} D^s T^s$, where D^s is a diagonal matrix, and T^s is a transformation matrix. In that case equation (4) becomes

$$\underline{p}^{s,e} \approx (T^s)^{-1} D^s T^s \underline{w}^e \quad (5)$$

so that

$$T^s \underline{p}^{s,e} \approx D^s T^s \underline{w}^e \quad (6)$$

Matrix T^s operating on $\underline{p}^{s,e}$ and \underline{w}^e maps these vectors into a basis where the accessible information matrix is diagonal. Because of the linearity of the integrals the same effect can be achieved if instead of using the usual L, M, and S cones, we used a set of “virtual” sensors obtained precisely by taking this linear combination T^s of the cone responses:

$$\underline{\rho}^{s,e} = T^s \underline{p}^{s,e} \quad \underline{\omega}^{s,e} = T^s \underline{w}^e \quad (7)$$

Then we can write, in terms of the virtual responses $\underline{\rho}^{s,e}$ and $\underline{\omega}^{s,e}$:

$$\underline{\rho}^{s,e} \approx D^s \underline{\omega}^{s,e} \quad (8)$$

Let us denote the i th component of the diagonal matrix D^s as r_i^s

$$\rho_i^{s,e} = r_i^s \omega_i^{s,e} \quad (9)$$

giving

$$r_i^s = \frac{\rho_i^{s,e}}{\omega_i^{s,e}} \quad (10)$$

Thus, by considering the virtual, recomposed sensors instead of the eye's actual LMS responses, (10) defines a biological reflectance notion analogous to the physicist's reflectance defined in (1) for each wavelength. For any surface, instead of having a reflectance function defined at every wavelength, we have a biological reflectance defined by three reflectance coefficients r_i^s , each being the ratio of reflected to incident light within one of the three virtual wavelength bands defined for $i=1,2,3$.

Here we see the link with Retinex theory, where Land (Land, 1964) proposed a similar definition of surface color. He called the sensor response triplet for light from a given surface divided by the triplet of responses for light from a perfect white reflectance (which is equivalent to taking the incident light itself) a *color designator*. The difference with Land is that Land used LMS responses, hoping that color designators would be approximately independent of illumination. PO however used responses of the recomposed virtual sensors defined for each surface by T^s .

The T^s found by PO will typically map the cone sensor functions into virtual sensors which have more concentrated support in certain wavelength regions: they are LMS type sensors but appear spectrally *sharper* than the cones. Because of this property they will more nearly have the property that the associated color designators are independent of illumination.

And here we see also the link to spectral sharpening. In spectral sharpening various algorithms are designed to make the reflectance term of (10) as independent of illumination as possible (Chong, Gortler, & Zickler, 2007; Finlayson, Drew, & Funt, 1994b). However, unlike the PO work, which returns biological color reflectance terms using a different transformation matrix T^s for each surface, spectral sharpening seeks a **single transformation for all surfaces and lights**. **One of the main contributions of this paper is to show that we can use a single, carefully chosen, transformation T and predict unique hue and color naming data equally well as the PO approach which used a per surface transformation T^s . Thus, and this is a significant improvement over the original work, we need not know the surface we are looking at in order to apply the theory.**

A second step in the PO formulation concerns their singularity index. PO calculated their PO biological reflectance coefficients for the set of Munsell chips used in the World Color Survey and noted that in certain cases, one or two of the three PO reflectance coefficients were close to zero. They called surfaces with this property "singular",

because they have the exceptional property of absorbing all light in one or two of the three bands defined by the virtual sensors. Such chips in some sense behave in a "simpler" fashion than other chips, because the variability of light reflected off them can be described within one or two bands, instead of needing three bands of light to describe, as is usually the case. **An implication of the biological reflectance triple having two zeros (or two values close to 0) is that under different lights only one of the virtual responses changes. For example a red surface with a biological reflectance triple of (1,0,0) implies a response under different lights of (k,0,0). That is, in the sense that variability is restricted to a plane or a line in 3-dimensional color space, one could say that such chips are in some sense more stable under changes of illumination, and might be easier to characterise, leading to being more frequently designated as focal.**

PO's singularity index took the biological reflectance triple \underline{r}^s and sorted its elements in descending order. It then calculated the 2-vector $\underline{\beta}^s$:

$$\beta_i^s = \frac{r_i^s}{r_{i+1}^s} \quad (i \in 1,2) \quad (11)$$

If k_1 and k_2 are respectively the maximum first and second beta components over a set of surfaces, PO's singularity index for a given surface was defined as:

$$S^{PO} = \max \left(\frac{\beta_1^s}{k_1}, \frac{\beta_2^s}{k_2} \right) \quad (12)$$

S^{PO} is large when one or more of the PO biological reflectance components are relatively very small. PO's hypothesis was that large singularity would correspond to colors that would be likely to be given a focal name in a given culture. Indeed, PO showed that this was the case: a strong correlation was found between the S^{PO} of (12) and the frequency with which colors in the WCS dataset are considered prototypical in different cultures. PO also extended their analysis to the question of unique hues and demonstrated that the singularity index could predict the position of the wavelengths for unique hues found classically in color psychophysics.

Spectral sharpening to define a more plausible biological model

The notion of spectral sharpening derives its roots from Land's retinex theory where there is a notion of *color designator* defined similarly to PO's notion of biological reflectance: The LMS triplet for an unknown surface un-

der unknown light is divided by the response of a white surface (under the same light). In so doing the intent (or hope) is that the light should “cancel” and the color designator should be illuminant independent. However, designators calculated for the original cone sensors are not optimally illuminant independent. Thus the technique of Spectral Sharpening is used to find a single transform of cone responses with respect to which color designators are as independent of the illuminant as possible. Such sensors have sensitivities that are more narrowly concentrated and less overlapping in the visible spectrum than those of the original cones. Spectrally sharpened color designators are similar to PO's notion of biological reflectance, except that a single transformation is used to create virtual responses, instead of having a different transform for each surface.

Expressed formally, spectral sharpening (Finlayson, Drew, & Funt, 1994a) seeks to find a single surface-independent sharpening transform T such that over all surfaces s :

$$\underline{p}^{s,e} \approx (T)^{-1} D^s T \underline{w}^e \quad (13)$$

which implies

$$\underline{p}^{s,e} = T \underline{p}^{s,e} \approx D^s T \underline{w}^e = D^s \underline{\omega}^e \quad (14)$$

Note that in contradistinction to PO all surfaces share the same sharpening transform (no dependency on s).

There is today a large literature on how to find the best transform T . In (Finlayson et al., 1994a) the starting point for sharpening was exactly the equation (14). There it was shown that if reflectance and illumination are respectively modelled by 2- and 3-dimensional linear models (or the converse) then (14) holds exactly. This is a remarkable result in two respects. First, using the statistical analysis provided by Marimont and Wandell (Marimont & Wandell, 1992) (that modelled light and reflectance by how they projected to form sensor responses) a 2-dimensional model for illumination and a 3-dimensional model for surface provides a tolerable model of real response data. Second, this result provides a strong theoretical argument for believing that a single sharp transform can be used for all surfaces. Other optimisation methods exist for deriving sharp sensors from Equation (14) including Data-based sharpening (Finlayson et al., 1994b), Tensor-based sharpening (Chong et al., 2007) and Sensor-based sharpening (Finlayson et al., 1994b). Figure 1 gives sharp sensors derived using these last 3 methods together with the Smith-Pokorny cone fundamentals (Smith & Pokorny, 1975).

It is clear from this figure that while the derived sensors are similar there is some variation in the results, raising the question of which sharp sensor set should be used. The question is not immediately easy to answer.

Indeed, the optimisations underlying the different sharpening techniques developed hitherto were, in part, formulated so that an optimal solution could be easily found. **None of the existing methods finds the sharp sensors which deliver the maximally illuminant-invariant color designators.**

Finding the optimal sharpening transform

Suppose we wish to compute the color designators (Land, 1964) for n reflectances viewed under a D65 illuminant where we map cone responses to sharp counterparts using the 3×3 sharpening matrix T . We calculate the designator for the s th surface:

$$\underline{\rho}^{s,D65} = T \underline{p}^{s,D65} \quad (15)$$

$$\underline{\omega}^{D65} = T \underline{w}^{D65} \quad (16)$$

Dividing (15) by (16) gives the color designator \mathbf{r}^s the components of which are:

$$\mathbf{r}_i^{s,D65} = \frac{\rho_i^{s,D65}}{\omega_i^{D65}} \quad (17)$$

In (17) the color designator has D65 in the superscript. This is because although we seek color designators which are illuminant independent we will not achieve perfect invariance. Rather as the illuminant varies so too will the computed designators. To select the sensors giving the best illuminant independence we will work with each sensor separately, that is, we will minimize each row of the matrix T individually (we denote each row as T_i).

Let us define a vector $\underline{v}_i^{D65} = [\mathbf{r}_i^{s_1,D65}, \dots, \mathbf{r}_i^{s_n,D65}]^t$ containing the designators defined in equation (17) for one of the sensors and a set of surface reflectances under the D65 illuminant, and let $\underline{v}_i^e = [\mathbf{r}_i^{s_1,e}, \dots, \mathbf{r}_i^{s_n,e}]^t$ be a vector containing the designators for the same surfaces and the same sensor under another illuminant e . The individual terms for both these vectors are the responses of a single sharp sensor divided by the responses of the light. As the illuminant changes we expect, for the best sharpening transform, that these vectors of designators will be similar to one another. Assuming m illuminants we seek the transform T which minimizes:

$$\min_{T_i} \frac{1}{m} \sum_{e=1}^m \frac{\| \underline{v}_i^{D65} - \underline{v}_i^e \|^2}{\| \underline{v}_i^{D65} \|^2} \quad i=1,2,3 \quad (18)$$

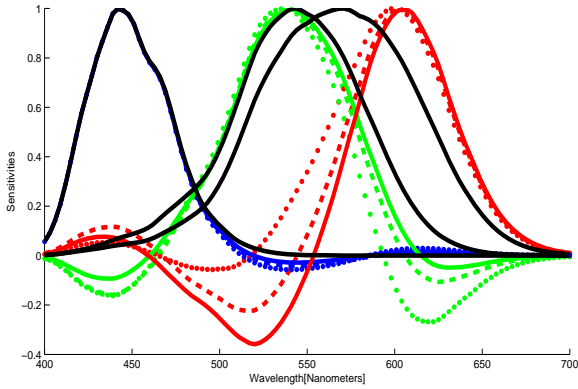


Figure 1: Sharpening sensitivities found by the different methods. Data-based sharpening (dashed line), Tensor-based sharpening (dotted line), and Sensor-based sharpening (continuous line). Cone fundamentals are plotted in black.

To find T we shall use the Spherical Sampling technique proposed by Finlayson and Susstrunk (Finlayson & Susstrunk, 2001). This method treats the sharpening problem combinatorially defining all possible reasonable sharpening transforms. Without recapitulating the detail, their key insight was that only if two sensors are sufficiently different (by a criterion amount) will it impact strongly on color computations. Indeed they argued that for spectral sharpening it suffices only to consider linear combinations of the cones resulting in sensors that are 1 or more degrees apart. Using this insight there is a discrete number of possible sensors and a discrete number of triplets of sensors. We simply take each of a finite set of sharp sensors and find the red, green, and blue sharp sensor that minimizes (18). The minimization was carried out using the WCS reflectances (a subset of 320 Munsell reflectances) and the same set of illuminants as in PO's paper (Chiao, Cronin, & Osorio, 2000), (Judd et al., 1964), (Romero, Garcia-Beltran, & Hernandez-Andres, 1997).

The optimal T transform we obtain starting with the Smith-Pokorny cone fundamentals (Smith & Pokorny, 1975) is:

$$T = \begin{pmatrix} 2.6963 & -2.3227 & 0.1559 \\ -0.6620 & 2.0651 & -0.3052 \\ 0.0543 & -0.0976 & 1.7924 \end{pmatrix} \quad (19)$$

In Figure 2 we plot the corresponding sharp sensors in solid red, green, and blue.

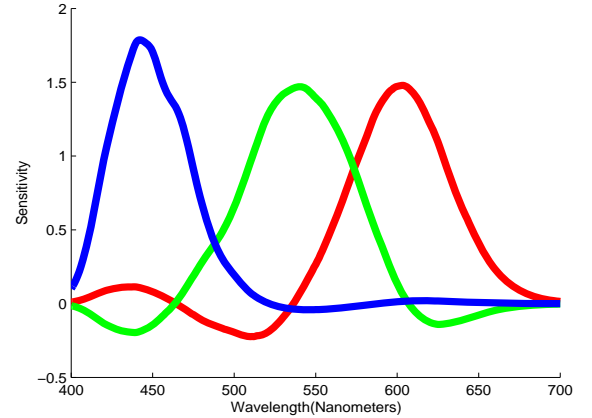


Figure 2: Sensors found using our approach.

Significantly, we find that PO biological reflectance functions (computed using a per surface transformation to virtual sensors) and the color designators (computed with respect to a single global sharpening transform) are strongly correlated (the correlation is 0.9917). Further we calculated the singularity index S^{PO} on the PO biological reflectances and the sharp color designators. These too are correlated (0.9251). While not identical these high correlations provide prima facie evidence that color designators calculated with respect to a single sharpening transform can be used instead of the per-surface biological reflectance functions proposed by PO (which are based on a per surface sharpening transform).

Compact singularity index

The idea of PO's singularity index was intuitively clear: they wished the index to be high when one or more of the color designator (or the PO biological reflectance) values is close to zero. However, to translate this idea into procedural form required sorting the designator values, calculating inter-band ratios, normalizing these ratios and taking a maximum. Here we suggest a more elegant, compact singularity measure, which will also turn out to have the advantage of being related to chromaticness.

Let us begin by writing three terms which measure the relative magnitude of one sensor response relative to the triplet of three responses. Here we use r , g , and b to denote the color designators calculated with respect to our sharp sensitivities (rather than r_1 , r_2 , and r_3). Further, let us begin by considering singularity in each color channel separately.

$$I_1 = \frac{r^3}{rgb} \quad (20)$$

$$I_2 = \frac{g^3}{rgb} \quad (21)$$

$$I_3 = \frac{b^3}{rgb} \quad (22)$$

By substituting test values into (20) through (22) we see each individual equation implements, correctly, a per channel idea of singularity. As an example, we can see that when $r \approx 0$ and g and b are $\gg 0$, then, I_2 and I_3 will be very large. We simply add these three terms together to define our new Compact Singularity Index:

$$S^C = I_1 + I_2 + I_3 = \frac{r^3 + b^3 + g^3}{rgb} \quad (23)$$

S^C computes a single measure which is large when the rgb designator has one or two values close to 0. Further, the function is symmetric with each of r , g and b playing the same role. That is, unlike the PO definition of singularity (see equations (11), (12)) we need not sort our sensor response or apply a maximum function.

Compact singularity and chromaticness

While (23) is simple (and as we shall see in the next section also provides a useful lens through which to view WCS color naming detail) it is interesting to examine its structure and to relate it to traditional color concepts. Let us modify our compact singularity index:

$$S^C = \frac{r^3 + b^3 + g^3}{rgb} \propto \frac{r^3 + b^3 + g^3}{rgb} - 3 \quad (24)$$

Then, we have

$$S^C \propto \frac{r^3 + b^3 + g^3}{rgb} - 3 = \frac{r^3 + b^3 + g^3 - 3rgb}{rgb} \quad (25)$$

In this form, the numerator intuitively gives us a measure of chromaticness: for achromatic surfaces, where $r=g=b$, the numerator will be 0 (note that, since we are dealing with designators, illumination effects have been canceled out). In contrast, for any chromatic surface the numerator will be positive, becoming bigger as we move away from the achromatic axis. Significantly, unlike tradi-

tional measures of saturation our chromaticness measure is unbounded: as the rgb becomes more and more saturated and the individual channel values go toward zero so our measure becomes unboundedly large.

Predictions and results

In one task in the World Color Survey, an average of 24 native speakers of each of 110 unwritten languages were shown a palette of 330 Munsell chips (see Figure 3) and asked to pick out the best (or “focal”) example(s) of the major color terms in their language. Figure 4 shows the histogram and a contour plot of the number of times a given chip was chosen as being such a “focal” color. It is seen that there are four peaks, corresponding to certain precise hues of “red”, “green”, “blue”, and “yellow”. Thus these four hues have a special status across a wide range of cultures.

A key idea in the PO work is that colors that have a high singularity index should correlate with colors frequently characterized as focal. The results of PO are shown on the left in Figure 5. From left to right the most kurtotic peaks correspond to “red”, “yellow”, “green”, and “blue” (see Figure 3). At each chip location, the singularity index for each surface is indicated. Clearly, the general trend of the data is quite similar to Figure 4: the singularity index increases and decreases in concert with the WCS histogram and the peaks are in similar positions.

In the present paper we have proposed two extensions of the PO work. First, we have calculated color designators with respect to a single sharpening transform (whereas in PO every surface has its own sharpening transform); second we have used our simplified Compact Singularity Index. The right hand histogram in Figure 5 plots our Compact Singularity Index with respect to the Munsell chips used in the WCS. As in PO, the singularity peaks are in close correspondence with the peaks of the WCS naming histogram. There is a somewhat better correspondence for “blue” compared to the predictions made by PO using their singularity index.

In their paper PO also compared their results to psychophysical experiments using “aperture colors”. “Aperture colors” are generated by sending lights with controlled spectral composition directly into the eye rather than by natural viewing of a colored surface. In order to make their approach compatible with the results of such experiments, and in particular in order to find a singularity index for lights instead of for surfaces, PO conjectured that the nervous system interprets light from aperture colors as though it corresponded to light coming from colored surfaces illuminated by white light. As referent for white light they chose D65.

Thus, when illuminated with D65 light, the Munsell chips used in the WCS can be considered to be aperture light sources whose coordinates can be plotted as points

in the usual CIE or LMS spaces. For each such light PO plotted the singularity of the corresponding Munsell chip, and observed that crests of singularity appeared in the CIE or LMS spaces, which, when extended out to the monochromatic locus, gave predictions for what should be the most singular monochromatic lights. These singular monochromatic lights corresponded very precisely to

the so-called “unique hues” observed in psychophysical measurements (see Table 1). The range of variation observed in existing experiments measuring unique hues could also be explained by the width of the areas of singularity defined by PO's procedure.

Figure 6 shows the results obtained when applying exactly the same method as PO to link aperture colors to Munsell chips, with the difference that we use our sharp sensors and our compact singularity index. In the left Figure we have a 3D plot of the singularity corresponding to 1600 Munsell chips (Joensuu, n.d.), each with the CIE value of the light it reflects when illuminated by D65 daylight. In the right part of the Figure we are looking at the x-y projection of the figure, and we have circled the four local maxima of the plot. We have connected these maxima to the neutral point, and extrapolated out to the monochromatic locus where we predict the unique hues should be. As seen in Table 1, our predictions are very close to PO's, and very close to the empirical data. The range of expected variation of the unique hues can be estimated in our approach by taking the range over which our compact singularity index exceeds some threshold. The range shown in the Table is obtained using a threshold of 15% of the maxima of each different mountain. It also corresponds accurately to the range of unique hues found in the empirical data. **However, we should note the existence of the Abney effect: there is some curvature in the lines of perceived hue in the chromaticity diagram. Therefore, our table shows an approximation of the hues.**

It is worth noting that in our approach, in contrast to PO's, there is a more direct method of obtaining unique hue predictions. Instead of extrapolating the LMS values of singular Munsell chips seen under white light out to the monochromatic locus, we can calculate directly the singularity of monochromatic lights. To do this, we again assume that the color designator associated with a light giving a particular sensor response is simply the designator of a surface illuminated by white light that would give that same sensor response. We can now get the designator associated with monochromatic lights by calculating the sharp sensor response to the monochromatic lights, and dividing by the sharp sensor response to white light. For this we have used D65 light. From the designator we can now calculate the singularity, using our compact singularity index. Figure 7 shows this index for all monochromatic lights. We see that there are extrema corresponding closely to the unique hues (see Table 1, last row) and in agreement with the more indirect method of calculation. It is interesting that the singularity in the green region is spread between about 520 and 535 nm.

PO were also able to explain hue cancellation phenomena in their paper. Hue cancellation quantifies the fact that the addition to a light that appears bluish, of a certain amount of light that appears yellowish produces a light that appears neither bluish nor yellowish, and the same for lights that appear reddish or greenish (Jameson & Hurvich, 1955). Note that, we are able to explain this

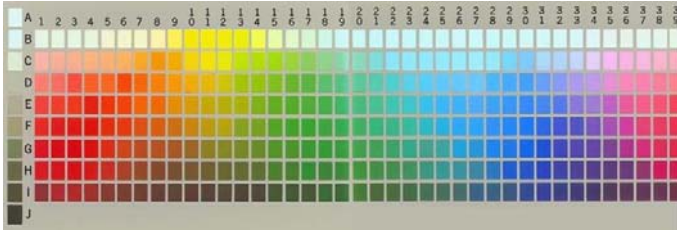


Figure 3: Munsell chips in the WCS data.

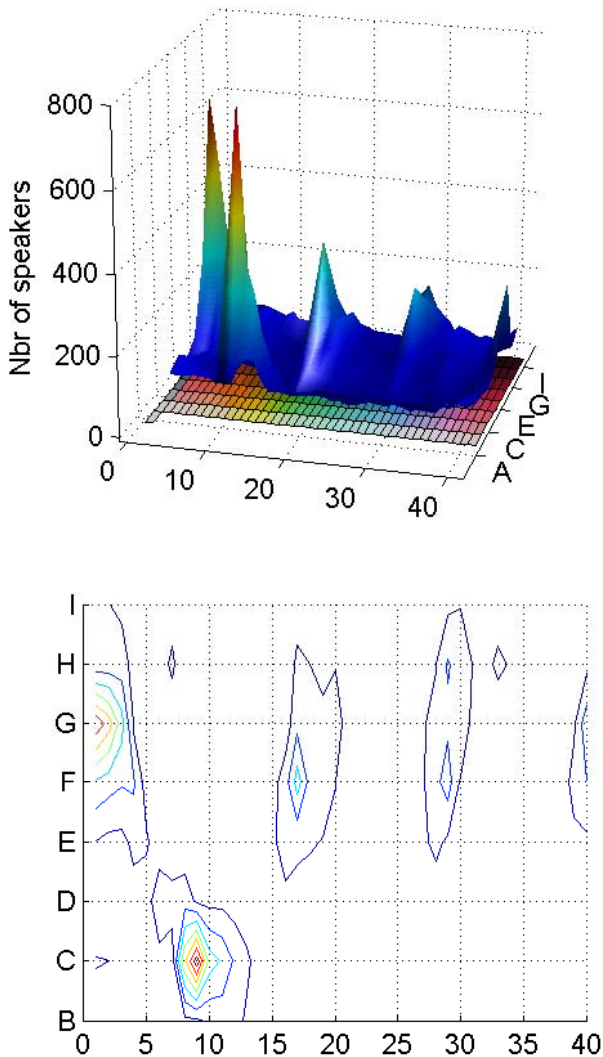


Figure 4: Psychophysical results of the WCS data.

data in the same manner PO did, by reference to the singularity of Munsell surfaces, transformed into CIE or LMS coordinates by illuminating them with white D65 light. But more interestingly, we are also able to explain the data as an opponent calculation from our spectrally sharp sensors.

First note that the relative peak sensitivity of our sensors is not fixed in all our previous computations (each sensor was derived independently). We can therefore adjust the peak sensitivities in order to fit the Jameson and Hurvich data. To this end, we have run an optimization to minimize the root mean square error between the Jameson and Hurvich data and our prediction. We do this minimization in two steps. First, we deal with the red-green cancellation by optimizing for $\alpha R - \beta G$. The optimal values we obtain are $\alpha = 0.56$ and $\beta = 0.77$. Second, with these values of α and β fixed, we move to the blue-yellow equilibrium, minimizing $\delta(\alpha R - \beta G) - (2\delta)\gamma B$. The $-(2\delta)\gamma$ term is defined in this way to have δ regarding the opponency and γ regarding the amplitude of the blue sensor. In this way, δ allows us to adapt the blue-yellow opponency away from the more usual $\delta = 1$. Following this approach we obtain $\gamma = 0.4860$.

In Figure 8 we can see the new sensor amplitudes and the resulting optimal prediction of the Jameson and Hurvich data, which has $\delta = 0.6477$, that is, the blue-yellow opponency is defined as $0.6477(R_c + G_c) - 1.2954B_c$ (already with the amplitude-corrected sensors R_c , G_c , B_c). The two cancellation curves show, on the one hand, the

intensity of a monochromatic yellow light that must be added to a bluish light so that the corresponding stimulus is on the locus defining a unique hue different from yellow or blue, and on the other hand the same thing for red and green lights.

Our final experiment deals with hue equilibrium. Thanks to our account of the loci of unique hues from singular surface reflection properties, we (as did PO) compare our results to the hue equilibrium experiment of Chichilnisky and Wandell (Chichilnisky & Wandell, 1999). In that experiment, Chichilnisky and Wandell looked for the region of the space where a sensation is neither bluish nor yellowish, and similarly, the region of the space where the sensation is neither reddish nor greenish. Figure 9 provides comparison of Chichilnisky and Wandell's data with the results using PO's approach (left graph), and with the results obtained using the Compact Singularity Index following the PO reflectance procedure (graph on the center). In these graphs the data symbols represent Chichilnisky and Wandell's data for subject *es* while the solid lines represent the predictions using estimations of unique hues shown in Table 1. We can see that our predictions are about as close to the experimental data as those obtained from PO's approach. Finally, predictions using unique hues found by sharp sensors are shown in the right graph.

		Unique	Yellow	Unique	green
Dataset	Subjects	Mean(nm)	Range(nm)	Mean(nm)	Range(nm)
Scheffrin	50	577	568-589	509	488-536
Jordan-Mollon	97	-	-	512	487-557
Volbrecht	100	-	-	522	498-555
Webster (a)	51	576	572-580	544	491-565
Webster (b)	175	580	575-583	540	497-566
Webster (c)	105	576	571-581	539	493-567
Po's SI prediction	-	575	570-580	540	510-560
Our-model reflectances	-	580	570-585	555	540-565
Our model-sharp sensors	-	588	585-595	536	515-545
		Unique	Blue	Unique	Green
Dataset	Subjects	Mean(nm)	Range(nm)	Mean(nm)	Range(nm)
Scheffrin	50	480	465-495	-	-
Jordan-Mollon	97	-	-	-	-
Volbrecht	100	-	-	-	-
Webster (a)	51	477	467-485	EOS	-
Webster (b)	175	479	474-485	605	596-700
Webster (c)	105	472	431-486	EOS	-
Po's SI prediction	-	465	450-480	625	590-EOS
Our-model reflectances	-	470	460-480	615	600-EOS
Our model-sharp sensors	-	464	454-470	607	600-640

Table 1: Unique hues found in the different experiments and the prediction from our model: A new sensor basis along with the new CSI index. EOS means End Of Spectrum.

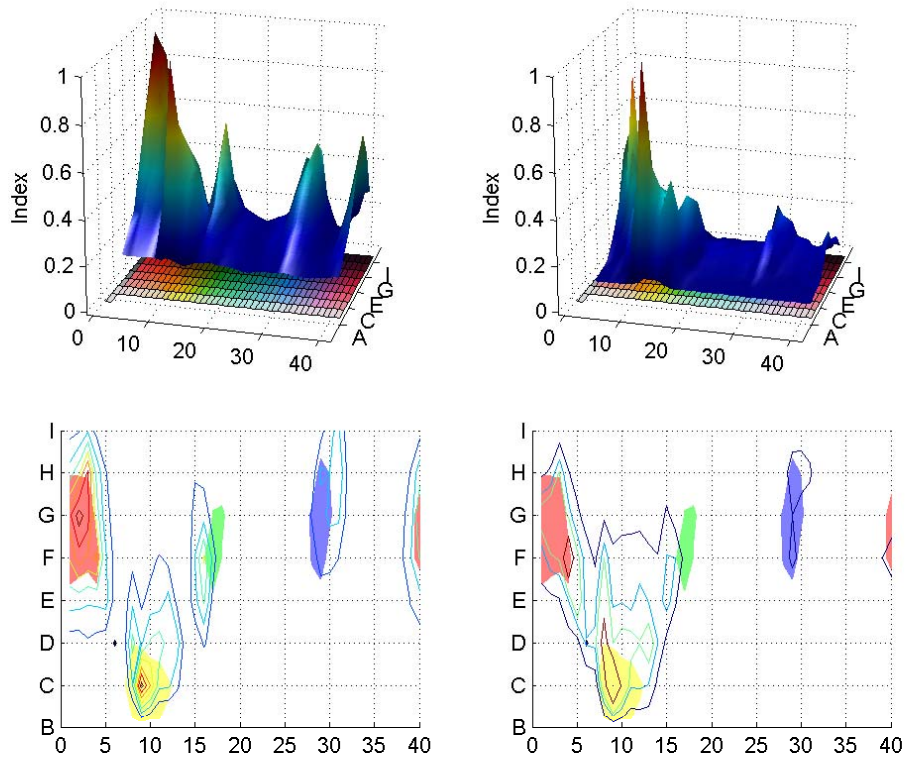


Figure 5: Comparison between the results obtained by PO in their paper (left) and our results using a single global sharpening transform T and the compact singularity index (right). The solid patches of the bottom-plots represent the top 10% of the WCS data.

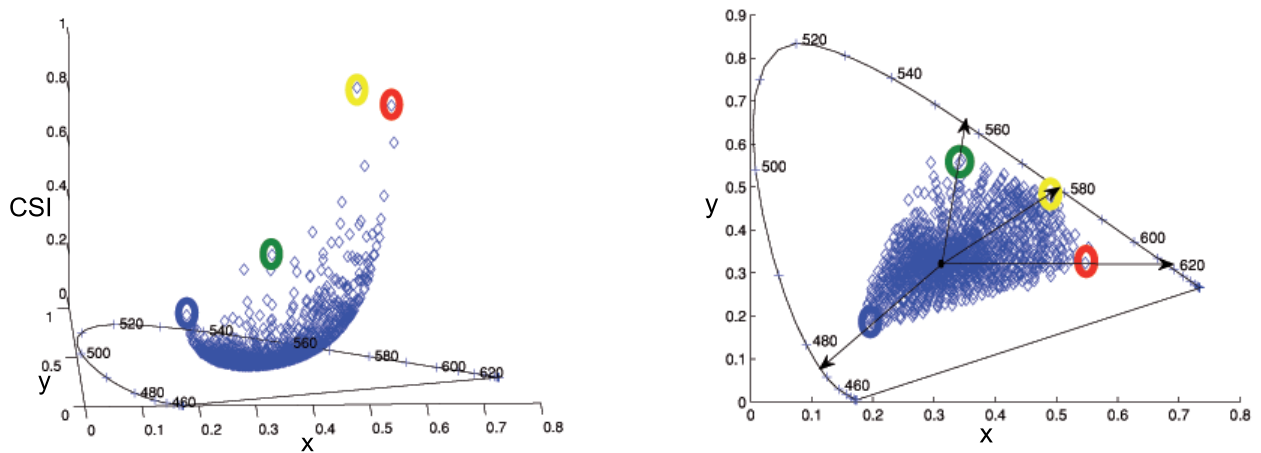


Figure 6: Left: Plot in x, y space for our new compact singularity index for the 1600 Munsell chips. Right: Projection of the compact singularity index and the locus of monochromatic lights.

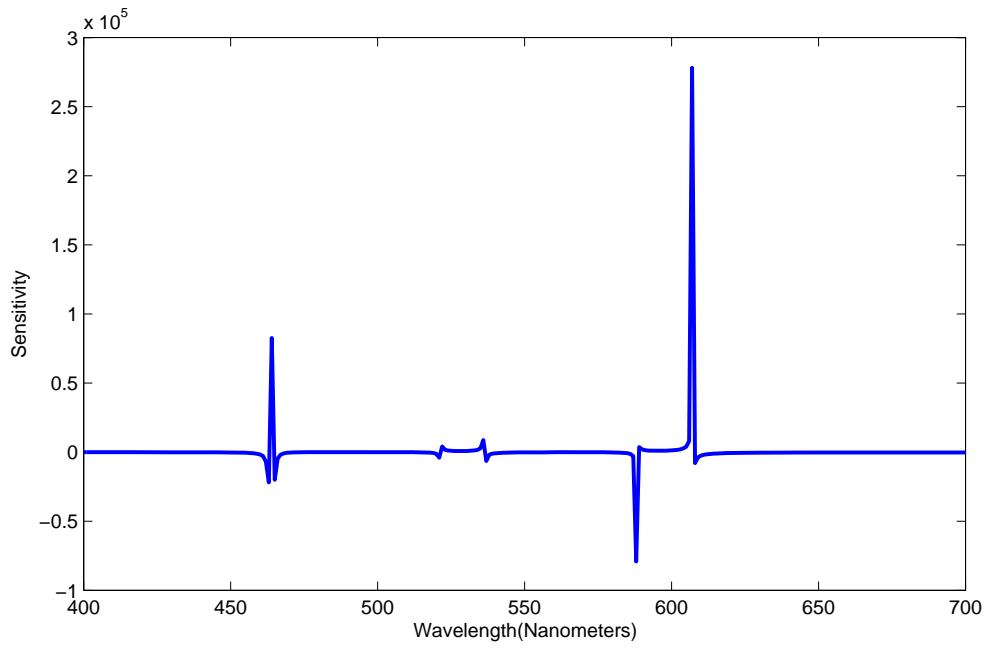


Figure 7 : Unique hues plot computed from the sharp sensors.

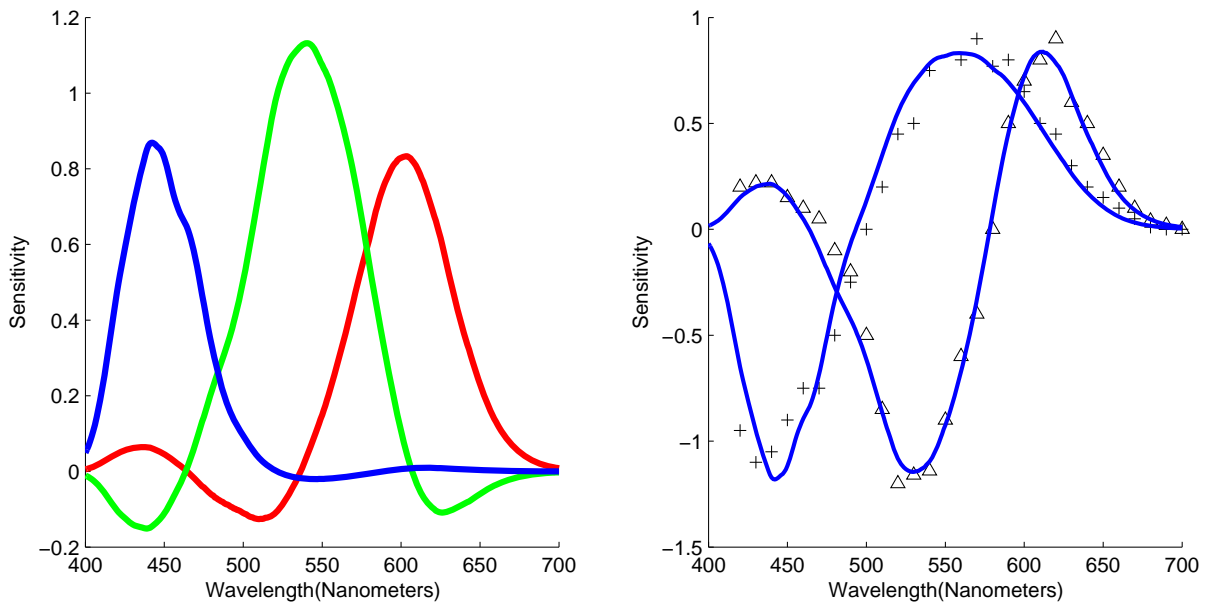


Figure 8: Hue cancellation prediction for our index. Left, the normalized sensors found to predict the data. Right, straight lines are our prediction (from an opponent conversion), data symbols represent Jameson and Hurvich data.

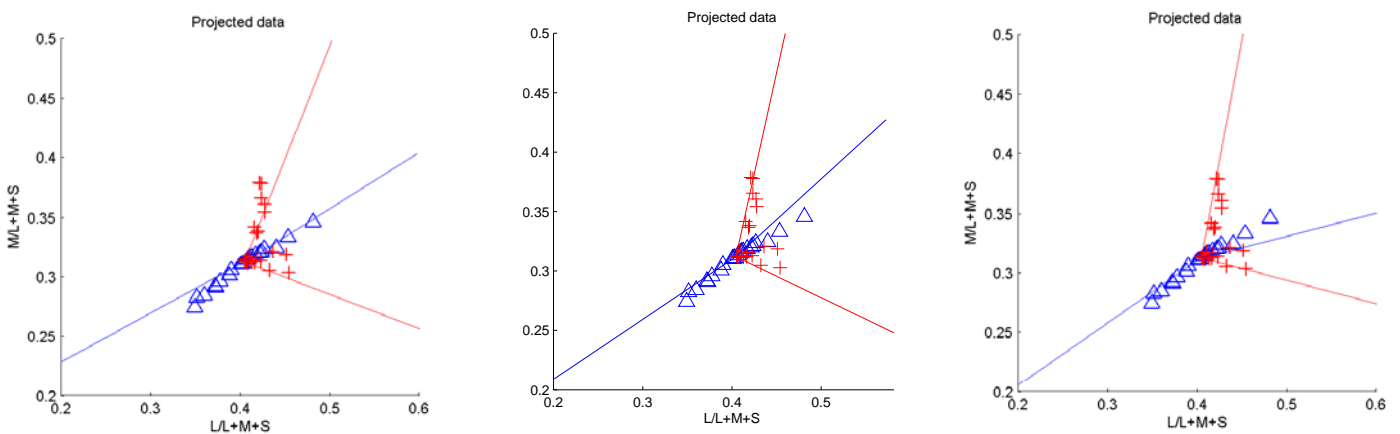


Figure 9: Hue equilibrium prediction. Left: PO singularity index. Center: Our compact singularity index with the reflectance procedure. Right: our compact singularity index with the sharp sensors approach. Crosses and triangles are the Chichilniski and Wandell data for their Subject es. Straight lines represent the estimations

Conclusions

PO suggested an interesting way of understanding psychophysical data on unique hues and anthropological data on cross-cultural color naming in terms of the linear mapping that describes how reflecting surfaces modify the LMS cone catches of the light that falls on them.

Their approach defined as “singular”, those surfaces that have the property that they project incoming LMS values into a **1- or 2-dimensional subspace of the 3-dimensional LMS space**. They showed that singular surfaces accurately correspond to surfaces in anthropological data that are most frequently considered prototypical in many cultures throughout the world. Singular surfaces are also those that, when illuminated with white light, accurately correspond to hues that appear to be pure or “unique”. Hue cancellation and opponent color matching is also accurately accounted for by PO's approach, without any parameter adjustments.

The main novelty of the present paper is to provide a way of interpreting PO's approach in terms of spectral sharpening theory. We show that by replacing the normal LMS sensors by a particular set of sharp sensors, PO's notion of singularity can be interpreted as corresponding to lights that activate only one or two, but not three of the sharp sensors. We show that a single, unique, set of sharp sensors satisfactorily accounts for all the data presented in PO's earlier work. In this way, we increase the biological plausibility of the model.

Importantly, in developing our new theory we define a new singularity index which is more compact than PO's and which establishes a clear link to the idea of chromaticness. Singular colors are colors which have high chromaticness on this measure. Our approach provides estimates of

color naming, unique hues, hue cancellation and opponent color matching which are as accurate if not more accurate than PO's.

Acknowledgements

Javier Vazquez-Corral and Maria Vanrell are grateful for support from TIN 2010-21771-C02-1 and Consolider-Ingenio 2010 CSD2007-00018 of Spanish MEC (Ministry of Science). K. O'Regan is partially financed by French ANR BINAHR. Graham Finlayson gratefully acknowledges support from EPSRC grant H022236.

References

- Berlin, B., & Kay, P. (1969). *Basic Color terms: Their universality and evolution*. Berkeley, CA: University of California Press.
- Burns, S. A., Elsner, A. E., Pokorny, J., & Smith, V. C. (1984). The Abney Effect - Chromaticity Coordinates of Unique and Other Constant Hues. *Vision Research*, 24(5), 479-489.
- Cicerone, C. M., Krantz, D. H., & Larimer, J. (1975). Opponent-Process Additivity .3. Effect of Moderate Chromatic Adaptation. *Vision Research*, 15(10), 1125-1135.
- Chiao, C. C., Cronin, T. W., & Osorio, D. (2000). Color signals in natural scenes: characteristics of reflectance spectra and effects of natural illuminants. *Journal of the Optical Society of America a-Optics Image Science and Vision*, 17(2), 218-224.

- Chichilnisky, E. J., & Wandell, B. A. (1999). Trichromatic opponent color classification. *Vision Research*, 39(20), 3444-3458.
- Chong, H. Y., Gortler, S. J., & Zickler, T. (2007). The von Kries hypothesis and a basis for color constancy. *2007 Ieee 11th International Conference on Computer Vision, Vols 1-6*, 2143-2150.
- Finlayson, G. D., Drew, M. S., & Funt, B. V. (1994a). Color Constancy - Generalized Diagonal Transforms Suffice. *Journal of the Optical Society of America a-Optics Image Science and Vision*, 11(11), 3011-3019.
- Finlayson, G. D., Drew, M. S., & Funt, B. V. (1994b). Spectral Sharpening - Sensor Transformations for Improved Color Constancy. *Journal of the Optical Society of America a-Optics Image Science and Vision*, 11(5), 1553-1563.
- Finlayson, G. D., & Susstrunk, S. (2001). Spherical sampling and color transformations. *Ninth Color Imaging Conference: Color Science and Engineering Systems, Technologies, Applications*, 321-325.
- Hering, E. (1891). *Zur Lehre vom Lichtsinne: Sechs Mittheilungen an die Kaiserliche Akademie der Wissenschaften in Wien*.
- Jameson, D., & Hurvich, L. M. (1955). Some Quantitative Aspects of an Opponent-Colors Theory .1. Chromatic Responses and Spectral Saturation. *Journal of the Optical Society of America*, 45(7), 546-552.
- Joensuu, U. o. (n.d.). Colour group. from spectral.joensuu.fi
- Judd, D. B., Macadam, D. L., Wyszecki, G., Budde, H. W., Condit, H. R., Henderson, S. T., et al. (1964). Spectral Distribution of Typical Daylight as Function of Correlated Color Temperature. *Journal of the Optical Society of America*, 54(8), 1031-1036.
- Kay, P. (2005). Color categories are not arbitrary. *Cross-Cultural Research*, 39(1), 39-55.
- Kay, P., & Regier, T. (2003). Resolving the question of color naming universals. *Proceedings of the National Academy of Sciences of the United States of America*, 100(15), 9085-9089.
- Kuehni, R. G. (2004). Variability in unique hue selection: A surprising phenomenon. *Color Research and Application*, 29(2), 158-162.
- Land, E. (1964). The retinex. *American Scientist*, 52, 247-264.
- Marimont, D. H., & Wandell, B. A. (1992). Linear-Models of Surface and Illuminant Spectra. *Journal of the Optical Society of America a-Optics Image Science and Vision*, 9(11), 1905-1913.
- Mollon, J., & Jordan, G. (1997). On the nature of unique hues. *John Dalton's Colour Vision-Legacy*, 54, 391-403.
- Parraga, C. A., Troscianko, T., & Tolhurst, D. J. (2002). Spatiochromatic properties of natural images and human vision. *Current Biology*, 12(6), 483-487.
- Philipona, D. L., & O'Regan, J. K. (2006). Color naming, unique hues, and hue cancellation predicted from singularities in reflection properties. *Visual Neuroscience*, 23(3-4), 331-339.
- Romero, J., Garcia-Beltran, A., & Hernandez-Andres, J. (1997). Linear bases for representation of natural and artificial illuminants. *Journal of the Optical Society of America a-Optics Image Science and Vision*, 14(5), 1007-1014.
- Smith, V. C., & Pokorny, J. (1975). Spectral Sensitivity of Foveal Cone Photopigments between 400 and 500 Nm. *Vision Research*, 15(2), 161-171.
- Valberg, A. (2001). Unique hues: an old problem for a new generation. *Vision Research*, 41(13), 1645-1657.
- Webster, M. A., Miyahara, E., Malkoc, G., & Raker, V. E. (2000). Variations in normal color vision. II. Unique hues. *Journal of the Optical Society of America a-Optics Image Science and Vision*, 17(9), 1545-1555.
- Wuerger, S. M., Atkinson, P., & Cropper, S. (2005). The cone inputs to the unique-hue mechanisms. *Vision Research*, 45(25-26), 3210-3223.
- Wyszecki, G., & Stiles, W. S. (1982). *Color science: concepts and methods, quantitative data, and formulae* (2nd ed.): John Wiley & Sons.
- Yendrikhovskij, S. N. (2001). Computing color categories from statistics of natural images. *Journal of Imaging Science and Technology*, 45(5), 409-417.